X-ray study of the charge-density-wave transition in single-layer TiSe_{2}

Xin-Yue Fang, Hawoong Hong, Peng Chen, and T.-C. Chiang

Phys. Rev. B **95**, 201409 — Published 16 May 2017

DOI: 10.1103/PhysRevB.95.201409

X-ray Vision of Charge-Density-Wave Transition in Single-Layer $TiSe_2$

Xin-Yue Fang,[1,2] Hawoong Hong,[3] Peng Chen,[1,2,4] and T.-C. Chiang[1,2,5]

[1]Department of Physics, University of Illinois at Urbana-Champaign, 1110 West Green Street, Urbana, Illinois 61801-3080, USA

[2]Frederick Seitz Materials Research Laboratory, University of Illinois at Urbana-Champaign, 104 South Goodwin Avenue, Urbana, Illinois 61801-2902, USA

[3]Advanced Photon Source, Argonne National Laboratory, 9700 South Cass Avenue, Lemont, IL 60439, USA

[4]Advanced Light Source, Lawrence Berkeley National Laboratory, 6 Cyclotron Road, Berkeley, CA 94720, USA

[5]Department of Physics, National Taiwan University, Taipei 10617, Taiwan

Abstract

Synchrotron x-ray studies of single-layer $TiSe_2$ reveal displacements of the Ti and Se atoms as a function of temperature. The measurements, with a high sensitivity of 0.001 Å, show a (2x2) charge density wave (CDW) structure at temperatures below a critical temperature of T_{C1} = 233 K. The temperature dependence follows a BCS-like second-order mean-field behavior. A five-layer $TiSe_2$ film also exhibits a CDW transition of the same character but at a lower transition temperature of T_{C5} = 204 K, which is the same as that for bulk $TiSe_2$. The results demonstrate that lattice distortion is an integral part of the CDW transition that must also involve renormalization of the electronic structure.

Recent advances in materials synthesis and processing have pushed the research frontier toward the two-dimensional (2D) limit of single atomic or molecular layers [1-3]. Such systems, when incorporated into devices, represent the ultimate miniaturization in thickness. Because of physical confinement of the electrons within the layer thickness, quantum effects are accentuated, potentially leading to enhanced or novel physical properties. A well-known example of 2D materials is graphene, which hosts unusual electronic features. The present study focuses on a single layer of $TiSe_2$. Like graphene, the bonding between $TiSe_2$ layers in the bulk crystal is of the van der Waals type, and a single layer is naturally stable and can be readily prepared. Unlike graphene, a single layer of $TiSe_2$ has a sizable band gap; it is thus a strong candidate as a versatile platform for next-generation bipolar electronics. A key scientific question is what the physical properties of such a single layer would be in relation to the bulk form. Bulk $TiSe_2$, like many other transition metal dichalcogenides, exhibits a CDW phase at low temperatures [4,5]. Such CDWs in bulk crystals have been under investigation for decades; still, controversies abound in regard to the physical origins of the transitions [6,7]. The transition temperature of bulk $TiSe_2$ is T_{CB} = 205 K, below which the lattice assumes a (2x2x2) distorted structure [8,9]. Our study of the single layer explores the presence or absence of a CDW transition associated with the lattice, and if there is one, the distortion pattern, the transition temperature, and the critical behavior near the transition. The physics of 2D CDWs can be expected to be different from the corresponding 3D cases because of the different dimensionality of the quantum mechanical interactions; furthermore, fluctuation effects associated with layer stacking in the bulk are absent in a single layer.

The most direct methods of extracting atomic positions in a crystal include x-ray and neutron diffraction [9]; the latter is, however, powerless for a single layer because of a lack of

sensitivity. While it is challenging to apply x-ray diffraction to a single layer because of a very small probing volume, this technique is arguably the most precise structural tool. Data analysis based on a kinematic formulation is straightforward and capable of yielding very accurate structural parameters. STM and low-energy-electron diffraction are capable of detecting structural transformations at the surface, but not below the surface, and it is difficult to extract quantitative information about atomic displacements especially at the 0.001-Å level.

The crystal structure of a single molecular layer of $TiSe_2$ in the normal phase is shown in Fig. 1(a). It consists of a Ti atomic layer sandwiched in-between two Se atomic layers, which together form a trilayer (TL). Each atomic layer in a TL is organized in a hexagonal lattice, and the Se atoms in the top and bottom layers are directly above or below alternate three-fold hollow sites of the Ti lattice. The bulk form of $TiSe_2$ in the normal phase adopts the 1T polymorph, which consists of TLs stacked directly on top of one another. The 3D Brillouin zone for the bulk crystal is shown in Fig. 1(b), and the 2D Brillouin zone for the single layer is realized by projecting the 3D prismatic zone into a hexagon in a plane.

Our x-ray diffraction measurements were performed at the surface x-ray scattering station, sector 33-ID-E, Advanced Photon Source, Argonne National Laboratory. A schematic diagram of the experimental configuration using a hexagonal surface coordinate system based on a six-circle geometry is shown in Fig. 1(c). The energy of the incident x-ray radiation was chosen to be 19.9 keV. The scattered radiation was detected by a Pilatus 100K area detector. Samples of 1- and 5-TL $TiSe_2$ were prepared by molecular beam epitaxy within the x-ray diffraction vacuum system [10]. A Si-terminated 6H-SiC(0001) wafer was used as the substrate. After degassing at 650 °C under ultrahigh vacuum for several hours, the substrate was flash annealed at 1300 °C briefly over multiple cycles to form a well-ordered bilayer graphene on the surface [11]. The

graphene termination leaves no dangling bonds on the surface. $TiSe_2$ overlayers were grown by co-deposition of Ti and Se onto the substrate maintained at 220°C under a high Se overpressure to avoid Ti clustering [1,12,13]. A calibrated thickness monitor was used to determine the amount of deposition [1,13]. The resulting overlayers were well ordered based on diffraction and showed an in-plane orientation parallel to that of the substrate, but the in-plane lattice constant is unstrained and incommensurate with respect to the substrate (the measured in-plane lattice constants for the graphene and $TiSe_2$ are 2.461 and 3.538 Å, respectively). The interfacial bonding is expected to be of the van der Waals type and very weak because of the incommensuration. For x-ray measurements with the sample at low temperatures, liquid nitrogen was used to cool the sample holder block. The sample was mounted on the holder block using metal straps to ensure good thermal contact. The temperature of the sample assembly was measured by a thermocouple mounted next to the sample. The chamber base pressure was 8×10^{-11} torr.

Figures 2(a) and 2(b) show normalized line scans along $\bar{\Gamma}-\bar{M}-\bar{\Gamma}$ in reciprocal space for the 1- and 5-TL samples, respectively, at temperatures ranging from ~140 to 290 K as indicated. Here, $\bar{\Gamma}$ and $\bar{M}$ are projections of Γ and M onto the basal plane [see Fig. 1(b)]. Each scan took 300 sec. The momentum transfer is (q, q, 0.2), where q ranges from 1.25 to 1.75, and the perpendicular momentum transfer 0.2 is chosen to be small for a stronger intensity. The scans for each sample show a peak at q = 3/2 that emerges and intensifies below transition temperatures T_{C1} and T_{C5}, respectively, for the two samples. This is a half-order peak corresponding to a (2×2) CDW phase. While the behavior appears similar for the two cases, T_{C1} and T_{C5} are different. For comparison, Figs. 2(c) and 2(d) show integral Bragg peaks at (1, 1, 0.2) for the 1- and 5-TL samples, respectively. By sharp contrast, these peaks do not show any appreciable changes

across the transition temperature (results not shown). The intensity of the half-order peak is very weak, about 0.5% of that of the corresponding integral Bragg peak, indicating very small atomic displacements associated with the CDW. Careful shielding of stray scattering during the experiment was essential to the observation of the half-order peaks. The widths of the Bragg and CDW peaks can be attributed to a mosaic spread and modulation effects caused by the incommensurate interface. The measured widths indicate a minimum coherence length of about 10 times the in-plane lattice constant.

Figure 3 presents for each sample the integrated (3/2, 3/2) peak intensity as a function of sample temperature obtained by direct data summation for q ranging from 1.25 to 1.75 with the background removed. There is a sharp onset at T_{C1} or T_{C5} followed by a continuous rise at lower temperatures, as opposed to a jump in intensity; the behavior is indicative of a second-order phase transition. The curves in Fig. 3 are fits based on a mean-field theory to be described below. The fits yield $T_{C1} = 232.6 \pm 0.8$ K and $T_{C5} = 204.0 \pm 1.0$ K. The errors are extracted from the data scattering only and do not include systematic errors. The sample temperature was determined during the experiment using a thermocouple; we estimate an absolute error of about ±0.5 K in addition to the data statistical error. Near and below the transition temperature, the intensity rise is expected to be linear for a second-order mean-field-type transition. The purple lines in Fig. 3 indicate the initial slopes and the linear power law near the onset. The measured T_{C5} is in close agreement with the known CDW transition temperature of bulk $TiSe_2$, $T_{CB} = 205$ K. The implication is that the CDW in a 5-layer film is essentially bulk-like [13].

Prior studies based on analytic modeling of the lattice dynamics [9,14-16] and first-principles calculations [1,13,17] have indicated a lattice instability in $TiSe_2$ that involves a symmetric triple-**q** soft mode at the zone boundary with the lattice distortion pattern shown in

Fig. 1(a), where the arrows indicate atomic displacements at $T = 0$ K, exaggerated by a factor of about 20. Each Ti (Se) atom is either stationary or displaces by $\delta\mathrm{Ti}$ ($\delta\mathrm{Se}$) along one of three symmetry-equivalent directions oriented at 120° apart. From a normal mode analysis (see supplementary document [18]), the Ti and Se displacements are related by the atomic mass ratio:

$$\frac{\delta\mathrm{Ti}}{\delta\mathrm{Se}} = 2\frac{m_{\mathrm{Se}}}{m_{\mathrm{Ti}}} \qquad (1)$$

The factor of 2 comes from the fact that there are two Se atomic layers, but just one Ti atomic layer, in a TL. A mean-field treatment of second-order phase transitions yields a universal functional form for the atomic displacements as a function of T. For the Ti atoms, its displacement is given by

$$\delta\mathrm{Ti}(T) = \delta\mathrm{Ti}(0)\tanh\left(A\sqrt{\frac{T_C}{T}-1}\right) \qquad (2)$$

The Se atomic displacement is described by a similar equation. Such mean-field equations also describe BCS superconductivity and many other second-order phase transitions, but the parameter A is system-specific. From Eqs. (1) and (2) and the known atomic scattering factors of Ti and Se, one can straightforwardly compute the x-ray scattering intensities, including the Debye Waller factor, for the fractional and integral order peaks, with $\delta\mathrm{Ti}(0)$ and A as parameters. The curves in Fig. 3 are best fits to the data under the constraint of experimentally observed intensity ratios of the factional- and integral-order peaks. The results yield $A = 1.18$, and the best $\delta\mathrm{Ti}(0)$ and other structural parameters are given in the supplementary document [19]. It happens that the (3/2, 3/2) peak is the most intense fractional order peak, and therefore it is chosen for the present analysis.

The Ti and Se atomic displacements as a function of temperature, shown in Fig. 4 as squares, are extracted from the experimentally determined fractional-order peak intensity using Eq. (1) and the parameters from the best fit. The curves are analytic results based on Eq. (2). Near the onset but with T below T_C, the atomic displacement varies as

$$\delta(T) \sim \sqrt{\frac{T_C}{T} - 1} \qquad (3)$$

The blue vertical dashed lines in Fig. 4 mark the transitions at T_{C1} and T_{C5} and, furthermore, emphasize the infinite slope at the onset, which allows for a precise determination of the transition temperature. The vertical scales in Fig. 4 and the data errors imply that the x-ray measurements have a sensitivity of ±0.001 Å.

Angle-resolved photoemission spectroscopy (ARPES) is another technique commonly employed to study CDWs. Prior work on ultrathin films of $TiSe_2$ have concluded that such films are semiconducting with a gap that widens below T_C, but the gap and the transition temperature are thickness dependent [1,13]. Furthermore, the experimental T_C based on ARPES converges to essentially the bulk limit already at a film thickness of 3 TLs [13]. Importantly, the values of T_{C1} and $T_{C5} = T_{CB}$ deduced from ARPES agree well with the present x-ray diffraction measurements. The gap variation based on ARPES also follows a second-order mean-field behavior. Because of the close correlation between the electronic structure and the atomic structure based on these experiments, we conclude that the CDW in $TiSe_2$ involves a tightly coupled electron-lattice system. ARPES, while sensitive to the electronic structure, does not provide structural information. The present study establishes that the lattice distorts in concert with the renormalization of the electronic structure for the CDW transition.

In retrospect, there has been a long raging debate in the literature about the origins of CDWs in various systems [20-22]. Traditional wisdom tends to put emphasis on the electronic structure as the driver for the transition [23,24]. In the present case, one could argue that a (2x2) lattice modulation in the single layer sets up a superlattice potential, which causes band folding and gap widening. The Se 4p valence band below the gap shifts down in energy, thus lowering the electronic energy, but this trend is counteracted by a rise in lattice strain energy. The net result is a (2x2) CDW, where the lattice and the electronic system evolve hand-in-hand to minimize the total free energy. The lower transition temperature for the five-layer film or the bulk material can be attributed to additional fluctuation effects associated with the third dimension that tend to suppress ordering [13,17].

In conclusion, our synchrotron x-ray studies of the atomic structure of single- and five-layer $TiSe_2$ as a function of temperature reveal details of the atomic displacement in connection with the CDW transitions. The transition temperatures are substantially different for the two films, with T_{C1} = 233 K and T_{C5} = 204 K, respectively, but the characters of the transition are otherwise the same. We conclude that, contrary to many existing models and theories, electronic effects alone cannot account for the CDW transition in $TiSe_2$. Lattice modulation is an integral part of the physics of CDWs.

Acknowledgments This work is supported by the U.S. Department of Energy (DOE), Office of Science (OS), Office of Basic Energy Sciences, Division of Materials Science and Engineering, under Grant No. DE-FG02-07ER46383. The Advanced Photon Source is supported by the Director, Office of Science, Office of Basic Energy Sciences, of the U.S. Department of Energy under Contract No. DE-AC02-06CH11357.

References

[1] P. Chen, Y. H. Chan, X. Y. Fang, Y. Zhang, M. Y. Chou, S. K. Mo, Z. Hussain, A. V. Fedorov, and T. C. Chiang, Nat. Commun. **6**, 8943 (2015).

[2] K. Sugawara, Y. Nakata, R. Shimizu, P. Han, T. Hitosugi, T. Sato, and T. Takahashi, ACS Nano **10**, 1341 (2016).

[3] P. Goli, J. Khan, D. Wickramaratne, R. K. Lake, and A. A. Balandin, Nano Lett. **12**, 5941 (2012).

[4] H. Cercellier, C. Monney, F. Clerc, C. Battaglia, L. Despont, M. G. Garnier, H. Beck, P. Aebi, L. Patthey, H. Berger, and L. Forro, Phys. Rev. Lett. **99**, 146403 (2007).

[5] K. Rossnagel, L. Kipp, and M. Skibowski, Phys. Rev. B **65**, 235101 (2002).

[6] M. Holt, P. Zschack, H. Hong, M. Y. Chou, and T. C. Chiang, Phys. Rev. Lett. **86**, 3799 (2001).

[7] T. E. Kidd, T. Miller, M. Y. Chou, and T. C. Chiang, Phys. Rev. Lett. **88**, 226402 (2002).

[8] K. Rossnagel, J. Phys. Condens. Matter **23**, 213001 (2011).

[9] F. J. Di Salvo, D. E. Moncton, and J. V. Waszczak, Phys. Rev. B **14**, 4321 (1976).

[10] H. Hong and T. C. Chiang, Nucl. Instrum. Methods Phys. Res., Sect. A **572**, 942 (2007).

[11] Q. Wang, W. Zhang, L. Wang, K. He, X. Ma, and Q. Xue, J. Phys. Condens. Matter **25**, 095002 (2013).

[12] J.-P. Peng, J.-Q. Guan, H.-M. Zhang, C.-L. Song, L. Wang, K. He, Q.-K. Xue, and X.-C. Ma, Phys. Rev. B **91**, 121113 (2015).

[13] P. Chen, Y. H. Chan, M. H. Wong, X. Y. Fang, M. Y. Chou, S. K. Mo, Z. Hussain, A. V. Fedorov, and T. C. Chiang, Nano Lett. **16**, 6331 (2016).

[14] J. A. Wilson, F. J. Di Salvo, and S. Mahajan, Phys. Rev. Lett. **32**, 882 (1974).

[15] S. S. Jaswal, Phys. Rev. B **20**, 5297 (1979).

[16] R. Bianco, M. Calandra, and F. Mauri, Phys. Rev. B **92**, 094107 (2015).

[17] P. Chen, Y. H. Chan, X. Y. Fang, S. K. Mo, Z. Hussain, A. V. Fedorov, M. Y. Chou, and T. C. Chiang, Sci. Rep. **6**, 37910 (2016).

[18] See Supplemental Material at [URL] for a detailed normal mode analysis for the soft phonon responsible for the charge density wave transition.

[19] See Supplemental Material at [URL] for a comparison of our experimental values of the atomic displacements with results from prior theoretical and experimental work where available.

[20] J. Ishioka, Y. H. Liu, K. Shimatake, T. Kurosawa, K. Ichimura, Y. Toda, M. Oda, and S. Tanda, Phys. Rev. Lett. **105**, 176401 (2010).

[21] Y. I. Joe, X. M. Chen, P. Ghaemi, K. D. Finkelstein, G. A. de la Peña, Y. Gan, J. C. T. Lee, S. Yuan, J. Geck, G. J. MacDougall, T. C. Chiang, S. L. Cooper, E. Fradkin, and P. Abbamonte, Nature Phys. **10**, 421 (2014).

[22] T. Pillo, J. Hayoz, H. Berger, F. Levy, L. Schlapbach, and P. Aebi, Phys. Rev. B **61**, 16213 (2000).

[23] D. Jérome, T. M. Rice, and W. Kohn, Phys. Rev. **158**, 462 (1967).

[24] W. Kohn, Phys. Rev. Lett. **19**, 439 (1967).

FIG. 1. (Color online) (a) Atomic structure of single-layer $TiSe_2$. Arrows indicate atomic displacements amplified by a factor of about 20 for the CDW phase at 0 K. (b) Bulk Brillouin zone with the hexagonal x-ray coordinate system indicated. (c) Experimental geometry for surface x-ray diffraction. The vectors k_{in}, k_{out}, and **q** represent the incoming and outgoing x-ray wave vectors and the momentum transfer, respectively.

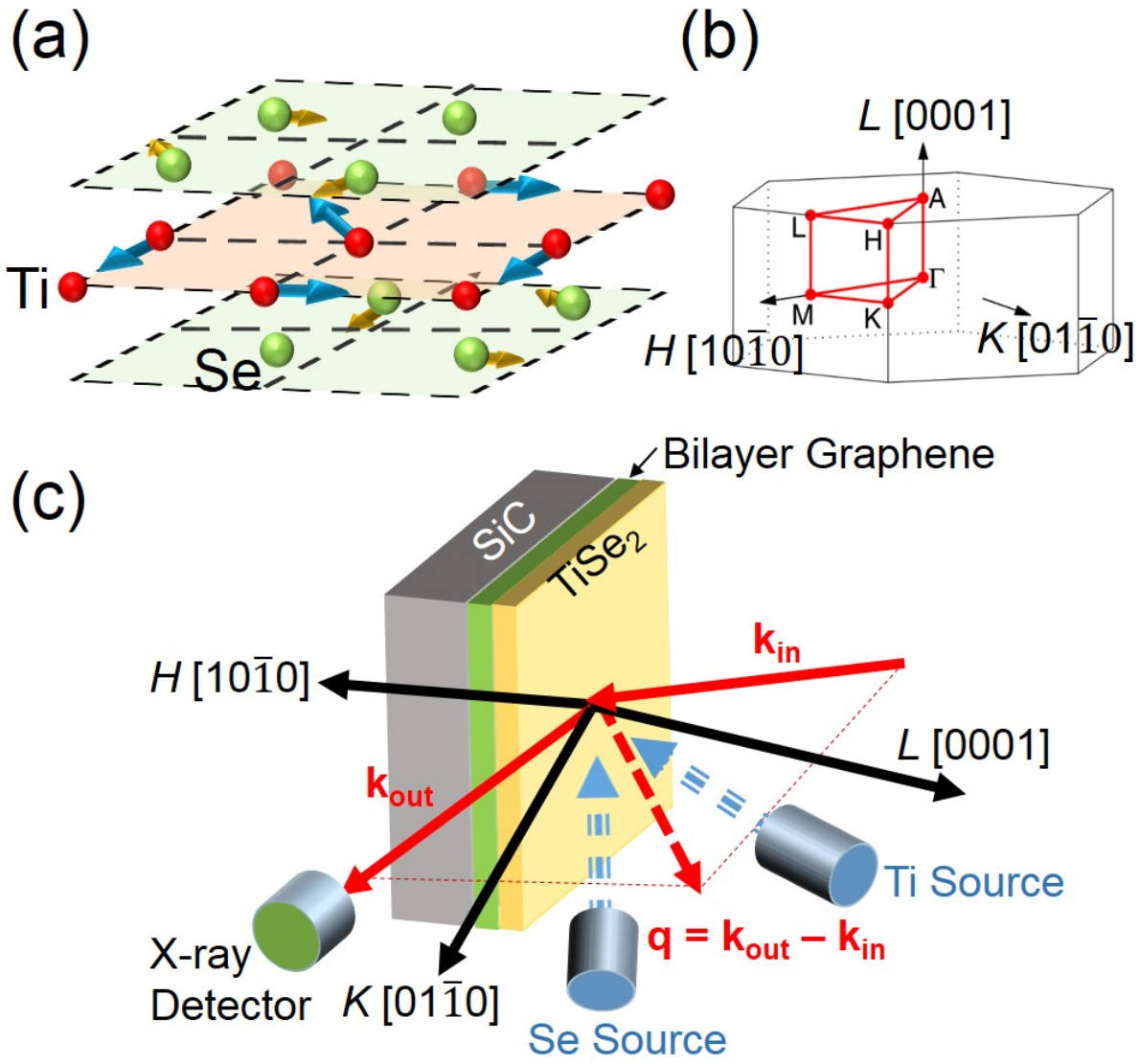

FIG. 2. (Color online) (a) Line scans in reciprocal space along $\bar{\Gamma}-\bar{M}-\bar{\Gamma}$ for single-layer $TiSe_2$. The momentum transfer **q** = (q, q, 0.2) is expressed in terms of reciprocal lattice units (r.l.u.). Data points are shown as squares and the curves are Gaussian representations. A fractional-order peak centered at q = 3/2 is seen at temperatures below the single-layer transition temperature T_{C1} = 233 K. (b) Similar results for a 5-TL sample. The transition temperature T_{C5} = 204 K is lower than the single-layer case. (c) Similar results for the (1, 1, 0.2) integral Bragg peak for the 1- and (d) 5-TL samples.

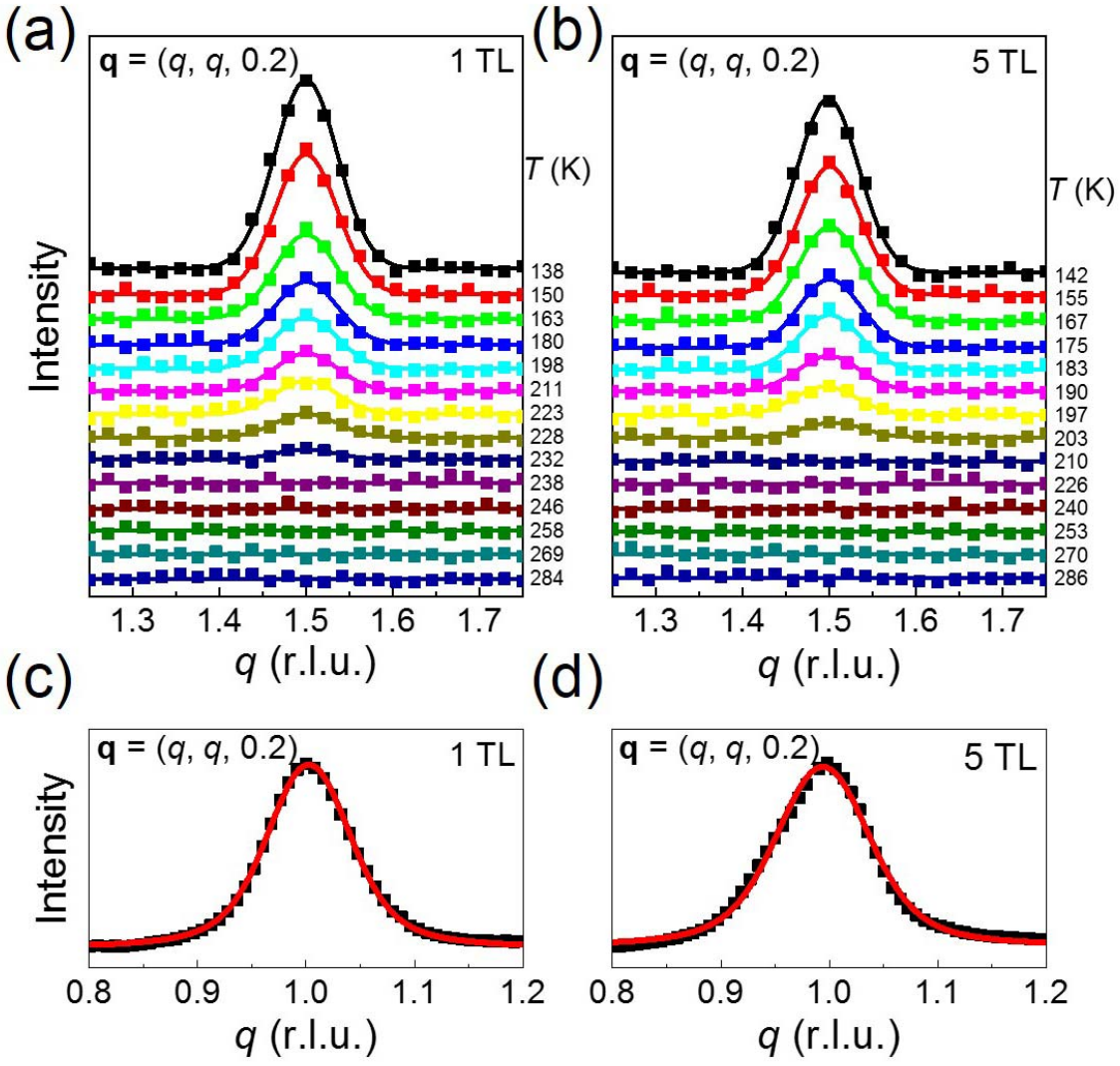

FIG. 3. (Color online) (a) Integrated intensity, indicated by squares, of the (3/2, 3/2, 0.2) peak as a function of temperature for a 1-TL sample. The green curve is a BCS mean-field fit. The blue dashed line indicates the transition temperature from the fit, and the purple line indicates the slope of the fitting function at the transition temperature. (b) Similar results for a 5-TL sample. The transition temperature is lower and agrees with the bulk transition temperature.

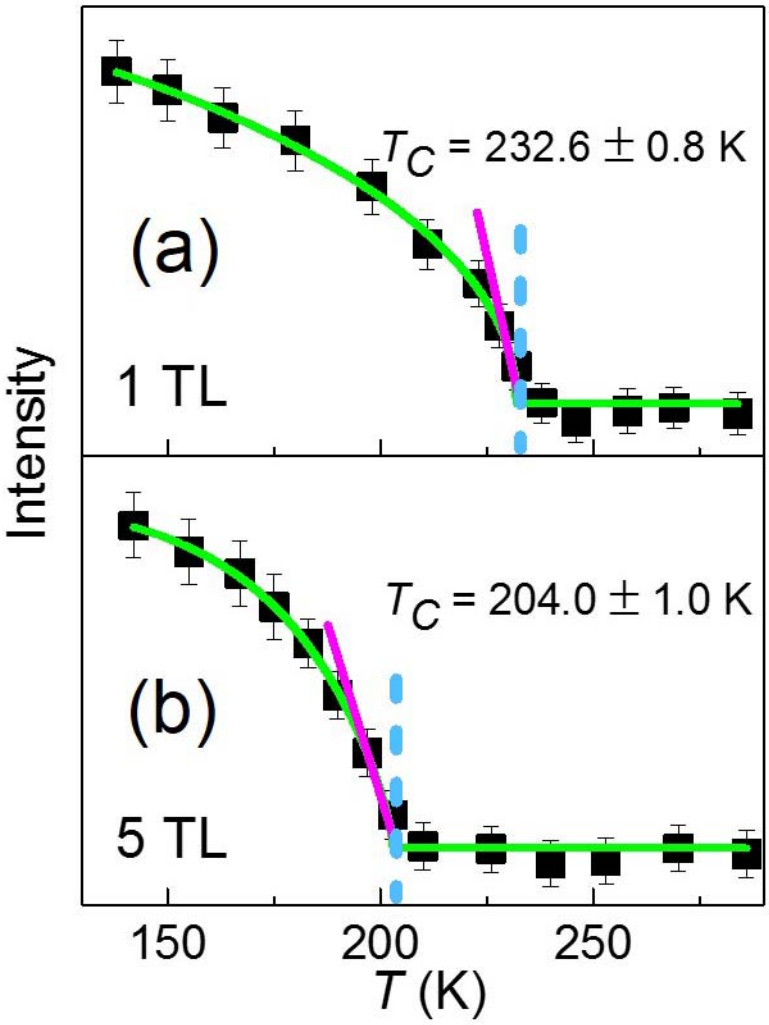

FIG. 4. (Color online) (a) Atomic displacement amplitude of Ti atoms, δTi, in Å as a function of temperature for 1- and 5-TL $TiSe_2$ extracted from the measured fractional-order peak intensity (squares) and deduced from the BCS fit (curves). Blue dashed lines indicate the transition temperatures. The slopes of the curves just below T_C are infinite. (b) Similar results for the Se atomic displacement amplitude, δSe.